Monochromatic neutrinos from scotogenic dark matter

Ricardo Cepedello, Pablo de la Torre, and Manuel Masip
Departamento de Física Teórica y del Cosmos Universidad de Granada, E-18071 Granada, Spain

(Received 18 May 2026; accepted 8 July 2026; published 27 July 2026)

The scotogenic model defines a framework for radiative neutrino masses and provides a viable dark matter candidate. Since the scotogenic dark matter is leptophilic, indirect searches appear as an especially interesting possibility. Here we discuss a variation of the usual model with a very distinct dark matter phenomenology. The scotogenic fermion singlets are naturally grouped into pseudo-Dirac pairs of mass of 0.1–1 TeV. We show that the lightest one constitutes a dark matter candidate that near threshold annihilates with a 90% branching ratio into neutrino pairs. The model gives the observed relic abundance consistent with the bounds from direct searches and with all neutrino and charged lepton data. We also show that, for a sub-MeV dark matter particle, the model suggests a scenario that could address the lithium problem.

DOI: 10.1103/7qfy-5w3v

I. INTRODUCTION: SCOTOGENIC DARK MATTER

A neutrino mass $m_\nu \approx 0.05$ eV implies a Wilson coefficient $c_\nu/\Lambda \approx (10^{15}\ \text{GeV})^{-1}$ in the Weinberg operator, suggesting that the UV completion of the neutrino sector involves physics at extremely high energies. We have, however, a compelling reason to hope for new physics at a more accessible scale: the dark matter (DM) of the Universe. Although one may argue that there are viable DM candidates of literally any mass, the weakly interacting massive particle (WIMP) paradigm has provided the simplest and most popular framework. A GeV–TeV stable particle produced thermally in the early Universe naturally implies the relic abundance deduced from observations, while its invisibility at the LHC and in direct searches favors models with stronger couplings to leptons than to quarks. Scenarios where the DM also completes the neutrino sector appear then as an interesting possibility.

In this context, the scotogenic model [1], also referred to as the leptophilic DM model or radiative seesaw model, has been extensively studied in the literature. The model is remarkable both because of its simplicity and its ability to explain neutrino masses and the DM relic abundance in a manner consistent with the lack of signals in direct, indirect, and collider searches [2–10]. It introduces a heavy (Majorana) fermion singlet N_i per light neutrino family and a second Higgs doublet $\eta = (\eta^+ \eta^0)$, both fields odd under an exact Z_2 matter parity that guarantees the stability of the lightest particle in this sector. In the basis of N_i and charged lepton (ℓ_α) mass eigenstates, the new interactions consistent with the symmetries read (in two-component spinor notation,[1] Lorentz and gauge indices contracted)

$$-\mathcal{L} \supset \sum_{i,\alpha}\left(\frac{1}{2}M_i N_i N_i + y_{\alpha i}\eta L_\alpha N_i + \text{H.c.}\right) + V(H,\eta), \quad (1)$$

with

$$\begin{aligned} V = &-\mu_1^2 H^\dagger H + \mu_2^2 \eta^\dagger\eta + \lambda_1 (H^\dagger H)^2 + \lambda_2 (\eta^\dagger\eta)^2 \\ &+ \lambda_3 (H^\dagger H)(\eta^\dagger\eta) + \lambda_4 (H^\dagger\eta)(\eta^\dagger H) \\ &+ \frac{\lambda_5}{2}[(H^\dagger\eta)^2 + \text{H.c.}], \end{aligned} \quad (2)$$

where a possible complex phase in λ_5 is absorbed in a redefinition of η. The lepton number assignment for the particles in this Lagrangian is given in Table I, implying that only the term proportional to λ_5 breaks L. Therefore, the coefficient in the Weinberg operator must be proportional to this parameter that can consistently be taken much smaller than the rest of the couplings. In particular, the loop diagram in Fig. 1 defines a radiative seesaw mechanism for the neutrino masses [11]. When the lightest Z_2-odd state is the fermion singlet N_1, then a relic density $\Omega_{N_1}h^2 \approx 0.11$ for $M_1 = 0.1-1$ TeV typically requires Yukawa couplings $y_1 = (\sum_\alpha |y_{\alpha 1}|^2)^{1/2} \gtrsim 0.1$, whereas neutrino masses $m_\nu \approx 0.05$ eV are obtained for $\lambda_5 \approx 10^{-9}$.

[1] $(\ell,\ \ell^c,\ N\ldots)$ are left and their conjugate $(\bar\ell,\ \bar\ell^c,\ \bar N\ldots)$ right spinors. We then define with primes Dirac $\ell'^T = (\ell\bar\ell^c)$ and Majorana $N'^T = (N\bar N)$ four-spinors, and $\eta^+\ell N + \eta^-\bar\ell\bar N = \eta^+\bar N' P_L \ell' + \eta^-\bar\ell' P_R N'$.

Published by the American Physical Society under the terms of the Creative Commons Attribution 4.0 International license. Further distribution of this work must maintain attribution to the author(s) and the published article's title, journal citation, and DOI. Funded by SCOAP³.

TABLE I. Lepton number in the original scotogenic model, with $L_\alpha = (\nu\ell)_\alpha$, $H = (h^+h^0)$, and $\eta = (\eta^+\eta^0)$.

ψ	L_α	e^c_α	N_i	H	η
$L(\psi)$	$+1$	-1	0	0	-1

In addition to coannihilations (e.g., $N_1\eta^+ \to \gamma e^+$), the dominant annihilation mode of N_1 in the early Universe is $N_1N_1 \to \ell^-_\alpha \ell^+_\beta, \nu_\alpha\bar{\nu}_\beta$ that goes through the diagram in Fig. 1 plus the corresponding u-channel contribution [12]. In the nonrelativistic regime, however, if we neglect lepton masses the cross section is p-wave suppressed: The initial state must be antisymmetric under exchange, so an orbital $\ell = 0$ implies $j = 0$ and thus a chirality flip in the final (anti)lepton. Expanding the cross section in powers of the relative DM velocity $\sigma v_{\rm rel} = a + bv^2_{\rm rel}$, we have [2,4]

$$a = 0; \quad b = \frac{M_1^2 y_1^4}{48\pi}\left[\frac{M_1^4 + m^4_{\eta^+}}{(M_1^2 + m^2_{\eta^+})^4} + \frac{M_1^4 + m^4_{\eta^0}}{(M_1^2 + m^2_{\eta^0})^4}\right]. \quad (3)$$

As a consequence, the dominant annihilation channel in astrophysical environments like the Sun or the Galactic Center, where $v_{\rm rel} \approx \sqrt{3T/M_1} \ll 1$, is $N_1N_1 \to L_\alpha \bar{L}_\beta V$ with $V = \gamma$, W, Z [13–16] (see Fig. 1).

As already mentioned, this scotogenic model has attracted a lot of attention during the past 20 years. Here we would like to discuss the DM implications of a simple variant that was proposed in the framework of the inverse seesaw mechanism [17–20]. It includes the same particle content but a different definition of lepton number, implying a very distinct DM phenomenology that may have been overlooked in previous literature.

II. THE MODEL

In the original scotogenic model, the singlets N_i have zero lepton number, and the inert doublet η is a scalar antilepton. The Yukawa couplings $y_{\alpha i}$ in Eq. (1) respect lepton number and are then unsuppressed, while the only coupling breaking L is $\lambda_5 \approx 10^{-9}$. Instead, we assume the presence of pairs (N_i, N^c_i) of fermion singlets with lepton number $+1$ and -1, respectively, together with a different assignment to η, $L(\eta) = 0$ (see Table II). In the limit of exact lepton number, a Majorana mass for the singlets and an interaction $\eta L_\alpha N_i$ are forbidden, whereas a Dirac mass, a λ_5 term in the scalar potential, and the Yukawa interaction $\eta L_\alpha N^c_i$ are all allowed. Let us consider the model with just one (N, N^c) pair. Including the terms that break L, the Lagrangian reads

TABLE II. New lepton number assignment.

ψ	L_α	e^c_α	N_i	N^c_i	H	η
$L(\psi)$	$+1$	-1	$+1$	-1	0	0

$$-\mathcal{L} \supset \left(MNN^c + \frac{\mu}{2}NN + \frac{\mu'}{2}N^cN^c + \sum_\alpha (y_\alpha \eta L_\alpha N^c + \epsilon_\alpha \eta L_\alpha N) + \text{H.c.}\right) + V(H,\eta), \quad (4)$$

where $\epsilon_\alpha \ll y_\alpha$ and $\mu, \mu' \ll M$.

A. L-conserving limit

It is instructive to first consider the case with unbroken lepton number: $\epsilon_\alpha = 0 = \mu, \mu'$ and the two fermion singlets defining a Dirac fermion N' of mass M whose left- and right-handed components are N and $\bar{N}^c$, respectively.

(i) The first observation is that, obviously, the standard neutrinos ν_α stay massless as long as L is unbroken.

(ii) The second one, that two Dirac fermions N' can annihilate in an s wave into lepton-antilepton and neutrino-neutrino pairs. In contrast with the Majorana case [19], the initial state in $N'\bar{N}' \to L'_\alpha \bar{L}'_\beta$ (see Fig. 2, left) is not required to be antisymmetric. This first process is described by the operator $(\overline{N'}\gamma^\mu P_R N')(\overline{L'}_\alpha \gamma_\mu P_L L'_\beta)$ [21], with $N'^T = (N\bar{N}^c)$. As for $N'N' \to \nu_\alpha\nu_\beta$ (in Fig. 2, right, u channel omitted), it is now an L-conserving and unsuppressed process where both the initial and the final fermion pairs are in an s wave with total spin zero. Notice that, since the channel $N'N' \to \ell_\alpha \ell_\beta$ is forbidden by charge conservation, these neutrinos come without the corresponding charged leptons. In the usual four-component spinor notation the process is described by the dimension-eight operator $(H^\dagger \bar{L}'_\alpha P_R N')(H^\dagger \bar{L}'_\beta P_R N')$. The insertion in the η^0

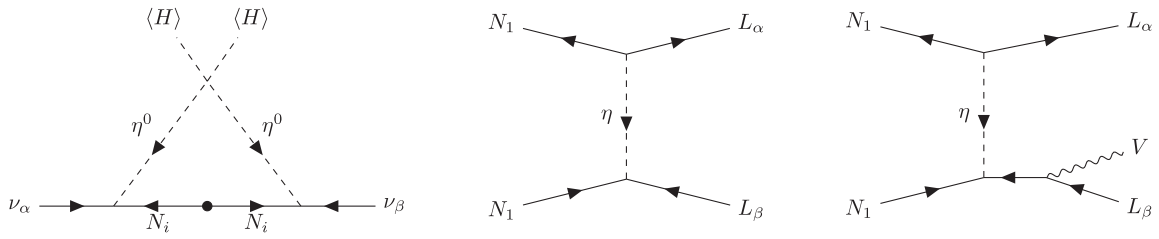


FIG. 1. Diagrams generating neutrino masses and DM annihilation.

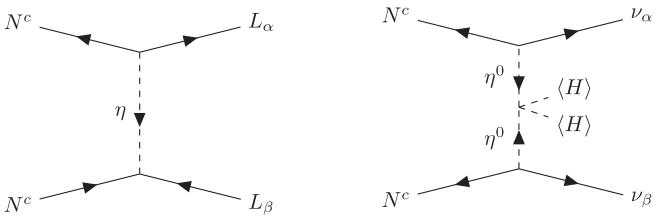


FIG. 2. Annihilation channels $N'\bar{N}' \to \nu_\alpha \bar{\nu}_\beta, \ell_\alpha \bar{\ell}_\beta$ (left) and $N'N' \to \nu_\alpha \nu_\beta$ (right).

line reflects the mass difference between $\mathrm{Re}\eta^0$ and $\mathrm{Im}\,\eta^0$,

$$m_R^2 - m_I^2 = \lambda_5 v^2, \tag{5}$$

whose contributions would exactly cancel if $\lambda_5 \to 0$. This would be the case in the usual scotogenic model when $M_1 \approx M_2$ [2]. Notice also that N^c couples to a single linear combination of the three neutrinos ν_α, with a coupling $y = \sqrt{|y_e|^2 + |y_\mu|^2 + |y_\tau|^2}$. The s-wave contribution to the total annihilation cross section of the Dirac singlet is then[2]

$$\begin{aligned} a_{N'N'\to\nu\nu} &= \frac{M^2 y^4}{256\pi}\left(\frac{1}{M^2+m_I^2} - \frac{1}{M^2+m_R^2}\right)^2 \\ &= a_{\bar{N}'\bar{N}'\to\bar{\nu}\bar{\nu}}, \\ a_{N'\bar{N}'\to L\bar{L}} &= \frac{M^2 y^4}{128\pi}\left(\frac{1}{M^2+m_I^2} + \frac{1}{M^2+m_R^2}\right)^2 \\ &\quad + \left(\frac{2}{M^2+m_{\eta^+}^2}\right)^2. \end{aligned} \tag{6}$$

(iii) The final observation is that flavor changing processes like $\mu \to e\gamma$ and $\tau \to e\gamma$ will be unsuppressed unless the electron Yukawa coupling to N^c is very small. These types of texture zeros could reflect a flavor symmetry and are necessary in any scotogenic model.

B. L-breaking effects

It is now straightforward to find the effects of the L-breaking terms in Eq. (1) on this Dirac model.

(i) Spectrum: The two components in the Dirac field separate into two Majorana fermions N_1, $N_{1'}$ of mass M_1 and $M_1 + \Delta M_1$, respectively. Let us be more specific and consider the case

$$-\mathcal{L} \supset \frac{1}{2}\begin{pmatrix} N & N^c \end{pmatrix}\begin{pmatrix} -\mu & M \\ M & -\mu \end{pmatrix}\begin{pmatrix} N \\ N^c \end{pmatrix}, \tag{7}$$

where, for simplicity, we have set $\mu' = \mu$ and have taken a negative Majorana mass coefficient ($\mu > 0$). The mass eigenstates are obtained after the unitary transformation

$$\begin{pmatrix} N_1 \\ N_{1'} \end{pmatrix} = \frac{1}{\sqrt{2}}\begin{pmatrix} 1 & 1 \\ i & -i \end{pmatrix}\begin{pmatrix} N \\ N^c \end{pmatrix}, \tag{8}$$

and the eigenvalues are $M_1 = M - \mu$ and $M_{1'} = M + \mu$, with $\Delta M_1 = 2\mu \lesssim 1$ MeV.

(ii) Neutrino masses and mixings: Both (quasi-Dirac) Majorana singlets inherit from N^c unsuppressed Yukawa couplings $y_{\alpha i}$ $(i = 1, 1')$ with the three lepton families:

$$\begin{aligned} -\mathcal{L} &\supset \eta(\, L_e \quad L_\mu \quad L_\tau\,)\begin{pmatrix} \epsilon_e & y_e \\ \epsilon_\mu & y_\mu \\ \epsilon_\tau & y_\tau \end{pmatrix}\begin{pmatrix} N \\ N^c \end{pmatrix} + \mathrm{H.c.} \\ &\approx \eta(\, L_e \quad L_\mu \quad L_\tau\,)\frac{1}{\sqrt{2}}\begin{pmatrix} \epsilon_e & -i\epsilon_e \\ y_\mu + \epsilon_\mu & i(y_\mu - \epsilon_\mu) \\ y_\tau + \epsilon_\tau & i(y_\tau - \epsilon_\tau) \end{pmatrix} \\ &\quad \times \begin{pmatrix} N_1 \\ N_{1'} \end{pmatrix} + \mathrm{H.c.}, \end{aligned} \tag{9}$$

where we have set $y_e \approx 0$ to suppress flavor changing neutral currents (FCNCs) involving the electron. The mass matrix generated at one loop reads then

$$\begin{aligned} (m_\nu)_{\alpha\beta} &\approx \frac{M_1}{16\pi^2}\left((Y\cdot Y^T)_{\alpha\beta} + \frac{\Delta M_1}{M_1} Y_{\alpha 1'} Y_{\beta 1'}\right) \\ &\quad \times \left(\frac{m_R^2}{m_R^2 - M_1^2}\ln\frac{m_R^2}{M_1^2} - \frac{m_I^2}{m_I^2 - M_1^2}\ln\frac{m_I^2}{M_1^2}\right), \end{aligned} \tag{10}$$

where the dominant elements in $(Y\cdot Y^T)_{\alpha\beta} + \frac{\Delta M_1}{M_1} Y_{\alpha 1'} Y_{\beta 1'}$ are

$$\begin{pmatrix} 0 & \epsilon_e y_\mu & \epsilon_e y_\tau \\ \epsilon_e y_\mu & (2\epsilon_\mu - \epsilon_M y_\mu) y_\mu & \epsilon_\tau y_\mu + \epsilon_\mu y_\tau - 2\epsilon_M y_\tau y_\mu \\ \epsilon_e y_\tau & \epsilon_\tau y_\mu + \epsilon_\mu y_\tau - 2\epsilon_M y_\tau y_\mu & (2\epsilon_\tau - \epsilon_M y_\tau) y_\tau \end{pmatrix}, \tag{11}$$

[2]We have evaluated vertices and amplitudes using SARAH [22,23], FeynArts [24], and FeynCalc [25,26].

with $\epsilon_M \equiv \Delta M_1/(2M_1)$. The matrix above defines a radiative inverse-seesaw mechanism for the neutrino masses [17–20]. It has a zero eigenvalue ($m_1 = 0$) but can fit the central value of the two neutrino mass differences and the two larger mixings. For θ_{13}, it implies

$$m_2 \cos^2\theta_{13} \sin^2\theta_{12} - m_3 \sin^2\theta_{13} = 0, \tag{12}$$

and thus, $\sin^2\theta_{13} = (4.55 \pm 0.20) \times 10^{-2}$ versus the current best fit value $\sin^2\theta_{13} = (2.16 \pm 0.06) \times 10^{-2}$ [27]. This prediction is a consequence of taking $y_e \approx 0$ (to prevent FCNCs involving the electron) together with $y_{\mu,\tau} = O(0.1)$, and its correction requires that the model includes at least a second (N, N^c) pair (see next section).

(iii) Annihilations: The dominant channels of annihilation and coannihilation between the two quasidegenerate fermion singlets $(N_1, N_{1'})$ can be obtained from our results for the Dirac fermion N' in the previous subsection. In particular, for the s-wave processes we have

$$a_{N_1N_1}, \quad a_{N_{1'}N_{1'}} \simeq a_{N'N'}, \quad a_{N_1N_{1'}} \simeq a_{N'\bar{N}'}. \tag{13}$$

In environments with no $N_{1'}$ states, coannihilations will be absent, and the only two-body s-wave channel processes are

$$N_1N_1 \to \nu_\alpha\nu_\beta, \bar{\nu}_\alpha\bar{\nu}_\beta. \tag{14}$$

In this case, the electroweak bremsstrahlung $N_1N_1 \to L_\alpha \bar{L}_\beta V$ will typically account for 10% of all the annihilations.

(iv) Decays, inverse decays, and other $N_1 \to N_{1'}$ transitions: The one-loop diagrams in Fig. 3 generate a transition magnetic moment [at this point, we switch to four-spinors and omit the prime, e.g., $N_1'^T = (N_1\bar{N}_1) = N_1{}^T$ or $\ell'^T = (\ell\bar{\ell}^c) = \ell^T$]

$$\mathcal{L}_{\rm eff} \supset \frac{i}{2}\mu_{1'1}\bar{N}_{1'}\sigma^{\mu\nu}N_1F_{\mu\nu}, \tag{15}$$

with [2]

$$\mu_{11'} \approx -\frac{ey^2}{32\pi^2}\frac{M}{m_{\eta^+}^2}F\left(\frac{M^2}{m_{\eta^+}^2}\right), \quad F(x) = \frac{-x - \ln(1-x)}{x^2}. \tag{16}$$

This implies that the heavier Majorana decays $N_{1'} \to N_1\gamma$ with a partial width

$$\Gamma_\gamma \approx \frac{\mu_{11'}^2}{\pi}(\Delta M_1)^3. \tag{17}$$

$N_{1'}$ can also decay into neutrinos:

$$\Gamma_\nu \approx \frac{y^4}{960\pi^3}\left[\left(\frac{1}{m_I^2 - M_1^2} - \frac{1}{m_R^2 - M_1^2}\right)^2 + \left(\frac{1}{m_I^2 - M_1^2} + \frac{1}{m_R^2 - M_1^2}\right)^2\right](\Delta M_1)^5, \tag{18}$$

with the first term from $N_{1'} \to N_1\nu\nu, N_1\bar{\nu}\,\bar{\nu}$ and the second one from $N_{1'} \to N_1\nu\bar{\nu}$. Despite being a tree-level process, this channel is mediated by a dimension-six operator (versus the dimension-five electromagnetic transition) and is negligible for $\Delta M_1 \approx$ keV.

In astrophysical environments with a hot plasma at $T \gtrsim \Delta M_1$, $N_{1'}$ may be produced via inverse decays $N_1\gamma \to N_{1'}$ and in collisions with neutrinos and electrons. To estimate the relevance of the first process, we take a Boltzmann photon distribution and a nonrelativistic N_1,

$$\frac{{\rm d}n_\gamma}{{\rm d}E} \approx \frac{E^2}{\pi^2}e^{-E/T}, \qquad \sigma_\gamma \approx \frac{\pi^2}{E^2}\Gamma_\gamma\delta(E - \Delta M_1). \tag{19}$$

The rate of $N_1\gamma \to N_{1'}$ transitions is then

$$\Gamma_\gamma^{\rm tr} \approx \Gamma_\gamma e^{-\Delta M_1/T}. \tag{20}$$

If $y_e \neq 0$, the transition can also go through $N_1\nu_e \to N_{1'}\nu, N_{1'}\bar{\nu}$, and $N_1e \to N_{1'}e$. In the limit $M_1 \gg E > \Delta M_1$, the inclusive cross section is just

$$\sigma_{\nu_e} \approx \frac{|y_e|^2y^2(E - \Delta M_1)^2}{64\pi}\left(\frac{1}{(m_I^2 - M_1^2)^2} + \frac{1}{(m_R^2 - M_1^2)^2}\right), \tag{21}$$

and in environments with a ${\rm d}n_\nu/{\rm d}E$ number density of ν_e, the rate becomes

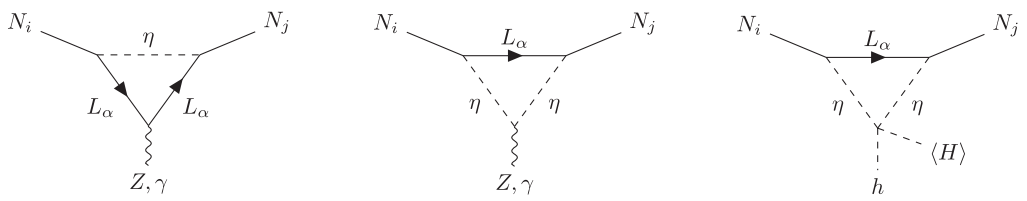


FIG. 3. Diagrams generating transitions and elastic collisions through the γ, Z, and Higgs portals.

$$\Gamma_\nu^{\rm tr} \approx \frac{|y_e|^2 y^2}{64\pi}\left(\frac{1}{(m_I^2-M_1^2)^2}+\frac{1}{(m_R^2-M_1^2)^2}\right) \times \int_{\Delta M_1}^{\infty} {\rm d}E \frac{{\rm d}n_\nu}{{\rm d}E}(E-\Delta M_1)^2. \quad (22)$$

For example, pp neutrinos at the solar core reach ${\rm d}n_\nu/{\rm d}E \approx 10^4\ {\rm cm}^{-3}\ {\rm keV}^{-1}$ at energies $E \leq 420$ keV. If $\Delta M_1 \leq 10$ keV, however, the number of thermal electrons with kinetic energy $E - m_e > \Delta M_1$ able to mediate the transition through $N_1 e \to N_{1'} e$ is much larger than the number of neutrinos, and

$$\sigma_e \approx \frac{|y_e|^4 m_e^2}{64\pi(m_{\eta^+}^2-M_1^2)^2}\sqrt{1-\frac{\Delta M_1}{E-m_e}}. \quad (23)$$

In a point inside the Sun with mass density ρ and temperature T, we have

$$\frac{{\rm d}n_e}{{\rm d}E} \approx \frac{3\rho}{m_p}\sqrt{\frac{4(E-m_e)}{\pi T^3}}e^{-(E-m_e)/T}, \quad (24)$$

implying

$$\Gamma_e^{\rm tr} \approx \int_{m_e+\Delta M_1}^{\infty} {\rm d}E \frac{{\rm d}n_e}{{\rm d}E} v_e \sigma_e \approx \frac{3\rho}{m_p}\frac{|y_e|^4 m_e^{3/2} T^{1/2}}{32\sqrt{2}\pi^{3/2}(m_{\eta^+}^2-M_1^2)^2} e^{-\Delta M_1/T}, \quad (25)$$

where we have taken $(\Delta M_1, T) \ll m_e$. From all these expressions, it follows, however, that in the Sun the $N_1 \leftrightarrow N_{1'}$ transitions involving electrons and neutrinos are negligible with respect to $N_{1'} \leftrightarrow N_1 \gamma$.

(v) Interaction with matter: Depending on their relative velocity $v_{\rm rel}$, the scattering of a DM particle N_1 off a nucleus A can be elastic ($N_1 A \to N_1 A$) or inelastic ($N_1 A \to N_{1'} A$). The inelastic collision is kinematically allowed only if [7]

$$\Delta M_1 < \frac{1}{2}\mu_{1A} v_{\rm rel}^2, \quad (26)$$

with $\mu_{1A} = M_1 m_A/(M_1+m_A)$. As shown in Fig. 3, these processes may be mediated by the photon, the Z boson, or the Higgs boson. In Table III, we summarize the different effective operators involved (we have used the Matchete package [21]).

TABLE III. Operators relevant for N_1-nucleus scattering ($i = 1, 1'$). V_q^Z and A_q^Z denote the vector and axial-vector quark couplings to the Z boson.

Operator	Elastic	Inelastic	Mediator
$(\bar{N}_i N_1)(\bar{q}q)$	S_{11}^h	$S_{1'1}^h$	h
$(\bar{N}_i \gamma^\mu \gamma_5 N_1)(\bar{q}\gamma_\mu(V_q^Z - A_q^Z\gamma_5)q)$	A_{11}^Z	$A_{1'1}^Z$	Z
$(\bar{N}_{1'} \gamma^\mu N_1)(\bar{q}\gamma_\mu(V_q^Z - A_q^Z\gamma_5)q)$	0	$iV_{1'1}^Z$	Z
$\bar{N}_i \gamma^\mu \gamma_5 N_1 \partial^\nu F_{\mu\nu}$	$\mathcal{A}_{11}$	$\mathcal{A}_{1'1}$	γ
$\bar{N}_{1'} \gamma^\mu N_1 \partial^\nu F_{\mu\nu}$	0	$ia_{1'1}$	γ
$\bar{N}_{1'} \sigma^{\mu\nu} N_1 F_{\mu\nu}$	0	$i\mu_{1'1}/2$	γ
$\bar{N}_{1'} \gamma^\mu N_1 A_\mu$	0	$ic_{1'1}$	γ

For elastic scattering, S_{11}^h and A_{11}^Z encode the one-loop effective interactions mediated by h and Z, respectively, while $\mathcal{A}_{11}$ denotes the electromagnetic anapole moment [28–31]. In the nonrelativistic limit [32–36], S_{11}^h implies a spin-independent N_1-nucleon contact interaction $V(x) = c_1^N \delta(\vec{x})$ with total cross section $\sigma_{\rm SI}^N = (\mu_{1N}^2/\pi)|c_1^N|^2$, where [4,9] $\mu_{1N} \equiv M_1 m_N/(M_1+m_N)$, $m_N = 0.94$ GeV,

$$c_1^N = \frac{f_N m_N y^2}{16\pi^2 m_h^2 M_1}\left(\lambda_3 \mathcal{G}_1(M_1^2/m_{\eta^+}^2) + \frac{\lambda_3+\lambda_4}{4}(\mathcal{G}_1(M_1^2/m_I^2)+\mathcal{G}_1(M_1^2/m_R^2))\right), \quad (27)$$

$\mathcal{G}_1(x) = [x + (1-x)\ln(1-x)]/x$, and $f_N = 0.3$ (we assume isospin-conserving scalar matrix elements).

The term proportional to $A_{11}^Z A_q^Z$ yields a spin-dependent contact interaction $V(\vec{x}) = c_4^N \vec{S}_{N_1} \cdot \vec{S}_N \delta(\vec{x})$ with total cross section $\sigma_{SD}^N = (3\mu_{1N}^2/(16\pi))|c_4^N|^2$. We obtain [4,9]

$$c_4^N = -\frac{y^2 a_N g}{16\pi^2 m_Z^2 c_W}\left((1-2s_W^2)\mathcal{G}_2(M_1^2/m_{\eta^+}^2) - \left(1+\ln\frac{m_R^2}{m_I^2}\right)\mathcal{G}_2(M_1^2/m_I^2)\right), \quad (28)$$

with $a_p = 0.677$, $a_n = -0.592$ [37], and $\mathcal{G}_2(x) = -1 + 2[x + (1-x)\ln(1-x)]/x^2$. The anapole interaction, in turn, leads to a velocity-suppressed scattering [4,33] that will be subleading in processes like direct detection or DM capture by the Sun.

Finally, in the same nonrelativistic limit, the elastic scattering $N_1 e \to N_1 e$ has a total cross section

$$\sigma_{\rm el}^e \approx \frac{3|y_e|^4 \mu_{Ne}^2}{64\pi(m_{\eta^+}^2-M_1^2)^2}, \quad (29)$$

with $\mu_{Ne} \approx m_e$. In contrast with quark scattering, this leptonic interaction arises already at the tree level, through the exchange of the charged component in the inert scalar doublet.

As for the inelastic processes, the dipole electromagnetic transition mediating $N_{1'} \to N_1\gamma$ and $N_1 e \to N_{1'} e$ has been already discussed in the previous paragraph. The inelastic upscattering $N_1 A \to N_{1'} A$ includes processes analogous to the elastic ones. Generically, these processes imply smaller nuclear recoils than the elastic ones and will introduce subleading effects in direct detection experiments. They can, however, play an important role in the DM capture by an astrophysical object: Despite this smaller recoil in the initial collision of N_1, the final decay $N_{1'} \to N_1\gamma$ adds $E_\gamma \approx \Delta M_1$ to the total energy lost by the projectile. The four transitions in Table III associated with bilinears that vanish for a single Majorana fermion ($\bar{N}_1\gamma^\mu N_1 = 0 = \bar{N}_1\sigma_{\mu\nu}N_1$) can also mediate inelastic spin-dependent and spin-independent interactions with a nucleus of atomic number Z, spin J_A, and magnetic moment μ_A (see [2] for a detailed evaluation of the cross sections).

III. DARK MATTER SCENARIOS

Some phenomenological aspects of the DM model proposed in the previous section depend critically on the mass difference $\Delta M_1 = M_{1'} - M_1$. Other observables, however, are insensitive to the particular value in the eV–MeV range of this parameter. In particular, the relic abundance is obtained at cosmological temperatures $T_{\text{f.o.}} \approx M_1/20 \gg \Delta M_1$. At these temperatures, the abundances of N_1 and $N_{1'}$ are very similar: The two Majoranas evolve as if they were a single Dirac fermion of mass M, and the final relic abundance could be estimated using the annihilation cross section in Eq. (6). We will, however, obtain a more precise estimate of $\Omega_{1,1'}h^2$ using micrOMEGAs [38,39] after implementing the model in SARAH [22] and generating the CalcHEP format files [40]. In our numerical computation, we will keep the full velocity dependence of the cross sections and will include all the relevant coannihilations with $N_{1'}$ and with the neutral and charged components in η [41].

Although the parameter space of the model is very wide, to illustrate its main features it may be useful to use benchmark points. We take three pairs of quasi-Dirac fermions $N_{i,i'}$ of masses $M_1 = 200$ GeV, $M_2 = 500$ GeV, $M_3 = 1$ TeV. We assume that the component N_i^c in each pair couples only to one lepton family (i.e., only $y_1 \equiv y_{e1}$, $y_2 \equiv y_{\mu 2}$, and $y_3 \equiv y_{\tau 3}$ are nonzero), while the N_i component in each pair couples to the three lepton families (all $\epsilon_{\alpha i}$ may be nonzero):

$$-\mathcal{L} \supset y_1 \eta L_e N_1^c + y_2 \eta L_\mu N_2^c + y_3 \eta L_\tau N_3^c + \sum_\alpha (\epsilon_{\alpha 1} \eta L_e N_1 + \epsilon_{\alpha 2} \eta L_\mu N_2 + \epsilon_{\alpha 3} \eta L_\tau N_3) + \text{H.c.} \tag{30}$$

The relic abundance depends then only on the coupling y_1 and on the spectrum of scalar mediators. Collider searches constrain the mass of the charged scalar: $m_{\eta^+} > 180$ GeV for $M_1 \ll m_{\eta^+}$ [42] or $m_{\eta^+} > 150$ GeV if $m_{\eta^+} - M_1 \leq 50$ GeV [43], whereas the bounds from $Z \to \eta_I^0 \eta_R^0$ are avoided if $m_I + m_R > m_Z$. In general, larger values of y_1 allow for heavier scalar mediators consistent with the observed value of the DM energy density. Notice also that in this model one can always keep m_{η^+} and m_R above the experimental bounds and then place m_I at the right distance from M_1 to obtain $\Omega_{1,1'}h^2$. This is in contrast to the usual scotogenic model, where λ_5 is very small, $m_I \approx m_R$, and all scalar mediators must have a mass above $M_Z/2$.

We take $y_1 = 0.4$, $m_{\eta^+} = 225$ GeV, $m_I = 211$ GeV, and $\lambda_5 = 0.7$, which correspond to $m_R = 296$ GeV (the masses have been calculated at the one-loop level [44] with SPheno [45]), and we obtain $\Omega_{1,1'}h^2 \approx 0.11$. Throughout our discussion, we will keep these values as default and set also $y_{2,3} = y_1$.

A second feature that is independent from the precise value of ΔM_1 is the N_1 elastic cross section off nucleons and electrons. Our benchmark gives

$$\sigma_{\text{el}}^e = 1.6 \times 10^{-45}\ \text{cm}^2, \qquad \sigma_{\text{SD}}^N = 2.5 \times 10^{-45}\ \text{cm}^2, \qquad \sigma_{\text{SI}}^N = 4.6 \times 10^{-48}\ \text{cm}^2. \tag{31}$$

As expected in scotogenic models, these cross sections are well below the limits established by direct search experiments. For the scattering with nucleons, we notice that the spin-dependent interaction is much larger than the spin-independent one. As for the elastic cross section with electrons, Eq. (29) reveals that it could be substantially larger in models where $m_{\eta^+} \to M_1$.

Next we fix the couplings $\epsilon_{\alpha i}$ that reproduce the central value of neutrino masses and mixings: $m_1 = 0.005$ eV, $m_2 = 0.01$ eV, $m_3 = 0.05$ eV, $\theta_{12} = 0.587$, $\theta_{23} = 0.819$, $\theta_{13} = 0.147$, and $\delta = 3\pi/2$. These masses and mixings can be obtained with different couplings $\epsilon_{\alpha i}$ (e.g., which will also depend on the particular value of ΔM_i). For example, if $\Delta M_i = 1$ keV for the three quasi-Dirac singlets we can take

$$\epsilon_{\alpha i} = 10^{-10} \times \begin{pmatrix} 12.4 & 0 & 0.18+0.18i \\ 0.24-0.27i & 5.6-0.02i & 0 \\ 0 & 0.89 & 2.0-0.02i \end{pmatrix}, \tag{32}$$

where we have taken three of the $\epsilon_{\alpha i}$ couplings to zero. Larger values of ΔM_i require either fine-tuning $\epsilon_{\alpha i}$ or smaller values of λ_5: When $\lambda_5 \to 0$, we recover the usual scotogenic model, with $\Delta M_1 \approx M_i$ and a total of six Majorana singlets. Our choice for the couplings $y_{\alpha i}$, with only one quasi-Dirac fermion pair sizeably coupled to each

lepton family, suppresses FCNCs almost to zero regardless of the value of ΔM_i. In particular [46],

$$\mathrm{BR}(\mu\to e\gamma)=\frac{3\alpha_{\mathrm{EM}}\mathrm{BR}(\mu\to e\nu_\mu\bar{\nu}_e)}{64\pi G_F^2 m_{\eta^+}^4}\times|y_1\epsilon_{\mu 1}F_2(M_1^2/m_{\eta^+}^2)+y_2\epsilon_{e2}F_2(M_2^2/m_{\eta^+}^2)|^2, \tag{33}$$

with $F_2(z)=(1/6-z+z^2/2+z^3/3-z^2\ln z)/(1-z)^4$. We obtain $\mathrm{BR}(\mu\to e\gamma)\approx 10^{-26}$ and similar branching ratios for $\tau\to e\gamma$ and $\tau\to\mu\gamma$.

Let us then sketch the different scenarios that are defined by the different values of ΔM_1. Again, to be definite we will comment just on four values of ΔM_1 that we consider representative.

(i) $\Delta M_1 = 0.2$ eV

These low values of the mass splitting imply an $N_{1'}$ lifetime similar to or larger than the age of the Universe. In the benchmark model that we have assumed, in particular, we have $\tau_{1'}=1.6\times 10^{10}$ yr. Both N_1 and $N_{1'}$ become then stable and are present with the same abundance in all astrophysical environments. The DM behaves in this case like an effective Dirac particle, and its main annihilation channels are into monochromatic neutrinos and electrons: $\nu_e\nu_e+\bar{\nu}_e\bar{\nu}_e+\nu_e\bar{\nu}_e$ (44%) and e^+e^- (55%).

(ii) $\Delta M_1 = 0.5$ keV

At this larger mass splitting, the assumed values of M_1 and y_1 imply $\tau_{1'}=1$ yr. In the early Universe, $N_{1'}$ decays before recombination, when the photon temperature is around 100 eV. The injected radiation of $E_\gamma=0.5$ keV will not affect the abundance of primordial nuclei or introduce CMB spectral distortions.

In astrophysical environments with $T\gtrsim\Delta M_1$, like the Sun's core, decays and inverse decays $N_{1'}\leftrightarrow N_1\gamma$ will keep similar abundances of both species. Again, in these conditions the DM becomes an effective Dirac particle that annihilates predominantly into monochromatic neutrinos and electrons. In contrast, in colder environments, $N_{1'}$ will be absent and N_1 will annihilate into $\nu_e\nu_e+\bar{\nu}_e\bar{\nu}_e$ (88%) and into three-body final states (e.g., $e^-\bar{\nu}W^+$).

(iii) $\Delta M_1 = 10$ keV

At these mass splittings, $N_{1'}$ will not be thermally produced, but for $v_{\mathrm{rel}}\approx 10^{-3}$ the $N_1\to N_{1'}$ transitions will be kinematically open in DM collisions with matter. As mentioned before, these inelastic processes will be subleading in direct search experiments, but they would contribute to the capture of DM by an astrophysical object like the Sun. Notice that, while in the elastic collision with a He nucleus, the energy lost by the incoming N_1 is always below $2m_{\mathrm{He}}v_{\mathrm{rel}}^2\approx 8$ keV, in inelastic collisions ($N_1\mathrm{He}\to N_{1'}\mathrm{He}\to N_1\gamma\mathrm{He}$) the final photon adds 10 keV to the total energy lost by the DM particle.

Like in the previous case, in any environment at $T<\Delta M_1$ the dominant annihilation channel will produce monochromatic neutrino pairs.

(iv) $\Delta M_1 = 100$ keV

In this regime, the N_1 to $N_{1'}$ transitions do not occur thermally or through collisions with low energy nuclei. In particular, the Sun will capture DM only via elastic scattering with nuclei and electrons. In our benchmark case, the elastic cross sections [in Eq. (31)] are very small, and thus the capture rate is weak; we estimate

$$C^e=5.6\times 10^{15}\ \mathrm{s}^{-1},\qquad C^{\mathrm{SI}}=1.9\times 10^{17}\ \mathrm{s}^{-1},\qquad C^{\mathrm{SD}}=2.8\times 10^{17}\ \mathrm{s}^{-1}. \tag{34}$$

The model, however, admits cases with much larger elastic cross sections. For example, if $M_1=60$ GeV, $y_1=0.38$, $m_I=78$ GeV, $m_R=437$ GeV, $m_{\eta^+}=308$ GeV, and $\lambda_5=3$, we obtain $\Omega_{1,1'}h^2=0.11$ and

$$\sigma_{\mathrm{el}}^e=2.4\times 10^{-48}\ \mathrm{cm}^2,\qquad \sigma_{\mathrm{SD}}^N=3.2\times 10^{-42}\ \mathrm{cm}^2,\qquad \sigma_{\mathrm{SI}}^N=3.9\times 10^{-48}\ \mathrm{cm}^2. \tag{35}$$

These spin-dependent and spin-independent cross sections are near the current bounds from direct searches [47], and they imply a much higher capture rate:

$$C^e=8.9\times 10^{13}\ \mathrm{s}^{-1},\qquad C^{\mathrm{SI}}=7.7\times 10^{17}\ \mathrm{s}^{-1},\qquad C^{\mathrm{SD}}=3.5\times 10^{21}\ \mathrm{s}^{-1}. \tag{36}$$

They induce a solar emission of $\Gamma_A=(C/2)\tanh^2(t_\odot/\tau)\approx 1.7\times 10^{21}$ neutrino pairs per second, or 3.9×10^{11} monochromatic neutrinos of $E=60$ GeV reaching Earth per km^2 and yr.

(v) $\Delta M_1 = 1.7$ MeV

This is an intriguing possibility, as the decay $N_{1'}\to N_1\gamma$ in the early Universe could affect big bang nucleosynthesis (BBN) [48,49]. More precisely, an injection of 1.58–2.22 MeV photons at $3\times 10^4\ \mathrm{s}\le t\le 10^6$ s ($T=1$–6 keV) would break the ^{7}Be ($^7\mathrm{Be}+\gamma\to{}^3\mathrm{He}+{}^4\mathrm{He}$) before it decays into ^{7}Li, while not affecting the primordial abundance of D or He. In our framework, it would require, first of all, a lighter DM particle, as the benchmark mass

$M_1 = 200$ GeV together with the relatively large values of ΔM_1 and $\mu_{1'1}$ imply a too short lifetime, $\tau_{1'} < 1$ s. For example, in a model with $M_1 = 10$ GeV and $y_1 = 0.07$, $m_I = 13$ GeV, $m_{\eta^+} = 495$ GeV and $m_R = 350$ GeV, the lifetime becomes $\tau_{1'} = 3 \times 10^4$ s.

The problem is, however, that to break a significant fraction of primordial ^{7}Be and solve the Li problem, we need a very large number density of decaying particles $N_{1'}$ [50], i.e., a very large final number density of DM particles. This implies that M_1 should be sub-MeV. Let us be a bit more specific and assume that $M_1 = 60$ keV, $M_{1'} = 3.8$ MeV, and $\tau_{1'} = 3 \times 10^4$ s. The sequence of events should go as follows: Both species are in thermal equilibrium with photons, electrons, and neutrinos until $T \approx 4$ MeV, when the abundance of the heavier partner goes down exponentially. Then, $N_{1'}$ freezes out when $n_{1'}/n_\gamma \approx 7 \times 10^{-7}$. The lighter species N_1, still in thermal equilibrium, becomes nonrelativistic during BBN, when its abundance drops exponentially until it decouples at $n_1/n_\gamma = 5 \times 10^{-5}$. This cold DM component will dominate the final N_1 energy density. The second component appears when $N_{1'}$ decays into $N_1\gamma$ at $T \approx 6$ keV. The 1.9 MeV photons then deplete most of the ^{7}Be (our parameter $\zeta_{N_{1'}\to\gamma} = n_{1'}E_\gamma/n_\gamma = 1.4 \times 10^{-6}$ sits at the lower edge of the viable region identified in [50]), whereas the ultrarelativistic N_1 fermions, once they are stopped by the expansion, will constitute around 1.3% of the total DM of the Universe.

IV. SUMMARY AND DISCUSSION

The search for DM has been a priority in the field, especially after the LHC completed the Standard Model with the discovery of the Higgs boson in 2012. Given the wide range of possibilities, it has been essential to identify generic features that may be shared by many models and can then guide the search. Within the WIMP paradigm, the scotogenic model has been very valuable, as it provides a framework to understand a leptophilic candidate. The model may look too simple or *ad hoc*, but the fact that it is based on symmetries brings technical consistency to a setup that is able to unify the neutrino and the DM sectors, indeed a remarkable feat. One could expect that any TeV model where the DM interacts with baryons only at the loop level and explains the tiny size of neutrino masses shares a similar phenomenology.

The scotogenic inverse seesaw model discussed here gives a complementary set of features and defines an also consistent playground for quasi-Dirac DM. It includes basically the same matter content as the usual model, but with a different lepton number assignment: Instead of $L(N_i) = 0$ and $L(\eta) = -1$, it has $L(N_i) = +1$, $L(N_i^c) = -1$, and $L(\eta) = 0$, with (N_i, N_i^c) becoming a pair $(N_i, N_{i'})$ of Majorana fermions with a mass splitting $\Delta M_i \ll M_i$. In the nonrelativistic limit, the DM annihilates predominantly into neutrino pairs: While in the original model $N_1N_1 \to \nu\nu$ is suppressed by lepton number conservation or $N_1N_1 \to \ell^+\ell^-$ is reduced by a factor of m_ℓ^2/M_1^2, in this setup the dominant annihilation channel is $N_1N_1 \to \nu\nu$ (the p-wave suppression in $N_1N_1 \to \ell^+\ell^-$ persists). We believe that this is the most striking feature of the model: It defines a UV complete framework where the WIMP may annihilate 90% of the time into monochromatic neutrinos. In contrast, the usual scotogenic model with two Majorana singlets of similar mass, a case often considered in the literature, implies that the annihilation of the lightest one near threshold is an electroweak bremsstrahlung (e.g., $N_1N_1 \to \ell^+\ell^-Z$).

Another interesting feature of the model is that it may behave very differently in astrophysical environments at different temperature. We have shown that in a hot plasma at $T \geq \Delta M_1$, decays and inverse decays $N_{1'} \leftrightarrow N_1\gamma$ keep similar abundances of the two species. In that case, the DM becomes an effective Dirac particle and the dominant annihilation channels include monochromatic neutrino and charged lepton pairs.

Monochromatic neutrinos can be searched for at km^3 telescopes in contained ν_e events. While the directionality in these events is very poor, the incident neutrino would deposit all its energy, and the telescope becomes a calorimeter with a much better energy resolution than in ν_μ events. In a particular DM model discussed before, we have estimated a solar flux of 3.9×10^{11} neutrinos per km^2 and yr, all of them at $E_\nu = 60$ GeV. If produced with the electron flavor (the case we have assumed), 55% of them will reach Earth with the same flavor. For comparison, the total flux of $E_\nu \geq 10$ GeV neutrinos from cosmic ray showers on the solar surface is 230 times smaller [51,52]. The atmospheric flux of electron neutrinos with energy 50 GeV $\leq E_\nu \leq$ 70 GeV within a circle of 10° radius around the Sun at zenith $\theta_z = -45°$ is 9×10^9 per km^2 and yr [53], suggesting that the model could be at the reach of KM3NeT [54] and IceCube [55]. Generically, the model provides solar fluxes more accessible at telescopes for scalar masses m_{η^+} closer to M_1 (that increase the capture rate via elastic collisions with electrons [56]), lower values of M_1 (implying a more effective capture via spin-dependent collisions with protons [57]), and lower values also of ΔM_1 (so that inelastic collisions with nuclei are above threshold).

We have finally discussed a possible scenario where the decay $N_{1'} \to N_1\gamma$ after BBN could break the primordial ^{7}Be before it decays into ^{7}Li. It would resemble the one proposed in [58], where a sterile MeV neutrino decays into a gamma plus a standard neutrino. In our model, the decay of $N_{1'}$ into the DM particle appears in a very narrow corner of the parameter space, where the general analysis in previous sections does not apply. Although it is then unclear whether the setup is flexible enough to actually

accommodate it, the potential link of the lithium problem to the origin of DM is very suggestive and may deserve a dedicated analysis.

In summary, several decades of direct and indirect searches have constrained substantially the parameter space of a DM WIMP. However, as long as there are possibilities still open, it seems worth identifying them and exploring them.

ACKNOWLEDGMENTS

We would like to thank Javier Fuentes-Martin, Renato Fonseca, and Manuel Pérez-Victoria for discussions. This work has been supported by the Spanish Ministry of Science, Innovation and Universities MICIU/AEI/10.13039/501100011033/ (No. PID2022-14044NB-C21), by Junta de Andalucía (No. FQM 101), and by Unión Europea-NextGenerationEU (No. AST22 8.4).

DATA AVAILABILITY

There are no publicly available research data or software supporting this manuscript. Requests for further information or data should be sent to the authors.

[1] E. Ma, Phys. Rev. D **73**, 077301 (2006).
[2] D. Schmidt, T. Schwetz, and T. Toma, Phys. Rev. D **85**, 073009 (2012).
[3] M. Garny, A. Ibarra, and S. Vogl, Int. J. Mod. Phys. D **24**, 1530019 (2015).
[4] A. Ibarra, C. E. Yaguna, and O. Zapata, Phys. Rev. D **93**, 035012 (2016).
[5] Y. L. Tang, Phys. Rev. D **97**, 035020 (2018).
[6] A. Beniwal, J. Herrero-García, N. Leerdam, M. White, and A. G. Williams, J. High Energy Phys. 06 (2020) 136.
[7] T. de Boer, R. Busse, A. Kappes, M. Klasen, and S. Zeinstra, J. Cosmol. Astropart. Phys. 08 (2021) 038.
[8] V. De Romeri, J. Nava, M. Puerta, and A. Vicente, Phys. Rev. D **107**, 095019 (2023).
[9] K. S. Babu, P. S. B. Dev, and A. Thapa, arXiv:2512.25035.
[10] A. Roy and R. Sahu, J. Cosmol. Astropart. Phys. 03 (2026) 014.
[11] Y. Farzan, S. Pascoli, and M. A. Schmidt, J. High Energy Phys. 03 (2013) 107.
[12] A. Ahriche, A. Jueid, and S. Nasri, Phys. Lett. B **814**, 136077 (2021).
[13] N. F. Bell, J. B. Dent, T. D. Jacques, and T. J. Weiler, Phys. Rev. D **78**, 083540 (2008).
[14] M. Garny, A. Ibarra, and S. Vogl, J. Cosmol. Astropart. Phys. 04 (2012) 033.
[15] N. F. Bell, A. J. Brennan, and T. D. Jacques, J. Cosmol. Astropart. Phys. 10 (2012) 045.
[16] K. Fukushima, Y. Gao, J. Kumar, and D. Marfatia, Phys. Rev. D **86**, 076014 (2012).
[17] T. Hambye, K. Kannike, E. Ma, and M. Raidal, Phys. Rev. D **75**, 095003 (2007).
[18] E. Ma, Phys. Rev. D **80**, 013013 (2009).
[19] K. Hikasa, Prog. Theor. Exp. Phys. **2024**, 083B02 (2024).
[20] N. T. N. Nga, N. H. Thao, and P. Van Dong, arXiv:2512.00854.
[21] J. Fuentes-Martín, M. König, J. Pagès, A. E. Thomsen, and F. Wilsch, Eur. Phys. J. C **83**, 662 (2023).
[22] F. Staub, Comput. Phys. Commun. **185**, 1773 (2014).
[23] A. Vicente, arXiv:1507.06349.
[24] T. Hahn, Comput. Phys. Commun. **140**, 418 (2001).
[25] R. Mertig, M. Böhm, and A. Denner, Comput. Phys. Commun. **64**, 345 (1991).
[26] V. Shtabovenko, R. Mertig, and F. Orellana, Comput. Phys. Commun. **207**, 432 (2016).
[27] I. Esteban, M. C. Gonzalez-Garcia, M. Maltoni, I. Martinez-Soler, J. P. Pinheiro, and T. Schwetz, J. High Energy Phys. 12 (2024) 216.
[28] C. M. Ho and R. J. Scherrer, Phys. Lett. B **722**, 341 (2013).
[29] J. Kopp, L. Michaels, and J. Smirnov, J. Cosmol. Astropart. Phys. 04 (2014) 022.
[30] J. Herrero-Garcia, E. Molinaro, and M. A. Schmidt, Eur. Phys. J. C **78**, 471 (2018).
[31] A. Ibarra, M. Reichard, and R. Nagai, J. High Energy Phys. 01 (2023) 086.
[32] A. L. Fitzpatrick, W. Haxton, E. Katz, N. Lubbers, and Y. Xu, J. Cosmol. Astropart. Phys. 02 (2013) 004.
[33] N. Anand, A. L. Fitzpatrick, and W. C. Haxton, Phys. Rev. C **89**, 065501 (2014).
[34] M. I. Gresham and K. M. Zurek, Phys. Rev. D **89**, 123521 (2014).
[35] E. Del Nobile, Phys. Rev. D **98**, 123003 (2018).
[36] R. Catena and B. Schwabe, J. Cosmol. Astropart. Phys. 04 (2015) 042.
[37] A. Airapetian *et al.* (HERMES Collaboration), Phys. Rev. D **75**, 012007 (2007).
[38] G. Belanger, F. Boudjema, A. Pukhov, and A. Semenov, Comput. Phys. Commun. **176**, 367 (2007).
[39] G. Alguero, G. Belanger, S. Kraml, and A. Pukhov, SciPost Phys. **13**, 124 (2022).
[40] A. Belyaev, N. D. Christensen, and A. Pukhov, Comput. Phys. Commun. **184**, 1729 (2013).
[41] K. Griest and D. Seckel, Phys. Rev. D **43**, 3191 (1991).
[42] S. Das, W. Howe, B. Shuve, D. Tucker-Smith, and R. Yager, Phys. Rev. D **112**, 055003 (2025).
[43] G. Aad *et al.* (ATLAS Collaboration), J. High Energy Phys. 06 (2023) 031.
[44] A. Goudelis, B. Herrmann, and O. Stal, J. High Energy Phys. 09 (2013) 106.
[45] W. Porod and F. Staub, Comput. Phys. Commun. **183**, 2458 (2012).
[46] T. Toma and A. Vicente, J. High Energy Phys. 01 (2014) 160.
[47] J. Aalbers *et al.* (LUX-ZEPLIN Collaboration), Phys. Rev. Lett. **135**, 011802 (2025).

[48] M. Pospelov and J. Pradler, Annu. Rev. Nucl. Part. Sci. **60**, 539 (2010).
[49] M. Kawasaki, K. Kohri, and T. Moroi, Phys. Rev. D **71**, 083502 (2005).
[50] V. Poulin and P. D. Serpico, Phys. Rev. Lett. **114**, 091101 (2015).
[51] P. de la Torre, M. Gutiérrez, M. Masip, and A. Oliver, Astrophys. J. **995**, 154 (2025).
[52] M. Masip, Astropart. Phys. **97**, 63 (2018).
[53] P. Lipari, Astropart. Phys. **1**, 195 (1993).
[54] S. R. Gozzini, EPJ Web Conf. **319**, 03003 (2025).
[55] R. Abbasi *et al.* (IceCube Collaboration), Phys. Rev. D **108**, 102004 (2023).
[56] T. T. Q. Nguyen, T. Linden, P. Carenza, and A. Widmark, Phys. Rev. D **113**, L101305 (2026).
[57] T. T. Q. Nguyen and T. Linden, arXiv:2602.15113.
[58] L. Salvati, L. Pagano, M. Lattanzi, M. Gerbino, and A. Melchiorri, J. Cosmol. Astropart. Phys. 08 (2016) 022.